# Paper II

II

## Low-loss, multimode 5-IDT SAW filter

J. Meltaus, V. P. Plessky, S. Härmä,
and M. M. Salomaa



J. Meltaus, V. P. Plessky, S. Härmä, and M. M. Salomaa, "Low-loss, multimode 5-IDT SAW filter", IEEE Transactions on Ultrasonics, Ferroelectrics, and Frequency Control, Vol. 52, No. 6, June 2005, pp. 1013-1019.

# Low-Loss, Multimode 5-IDT SAW Filter

Johanna Meltaus, Victor P. Plessky, *Senior Member, IEEE*, Sanna Härmä, and Martti M. Salomaa, *Member, IEEE*

***Abstract*—Longitudinally coupled resonator filters provide unbalanced-balanced operation with wide bandwidth, low loss, and high suppression levels. However, reducing the insertion loss in the 1.8–2.2 GHz range remains a challenging problem because at high frequencies the resistive losses arising from the relatively wide aperture of the filter may degrade the performance. A 5-interdigital transducer (IDT) filter has six gaps at which the periodicity of the grating is broken, resulting in additional loss due to scattering into the bulk. In this paper, we show that replacing the gaps between the transducers with short transducer sections having their pitch different from that of the main transducers reduces the insertion loss of the device. We present devices with balun operation at 1842 MHz with wide bandwidth of 4.5% and −40 dB suppression, with a minimum insertion loss less than 1 dB in the best devices, and a maximum insertion loss of −1.2 dB in the passband. The passband is quite flat, with <1 dB ripple. We also discuss the layout of the contact pads and the connections, and its effect on the device performance and balance characteristics.**

## I. Introduction

Longitudinally coupled resonator filters (CRF) [1]—often also referred to as dual-mode surface acoustic wave (SAW) filter (DMS) or multimode SAW filters (MMS)—recently have regained popularity as they enable a wide-band, low-loss response with high suppression levels and balanced operation. This is important for many emerging applications, especially when aiming for operation frequencies above 2 GHz. The size of CRFs is often smaller than that of ladder filters, and chip size can be reduced to $\sim 1.0 \times 0.6$ mm$^2$ for 2-GHz filters. At high frequencies, however, the resistive losses arising from the relatively wide aperture of CRFs may affect the performance. Losses due to the wide aperture can be reduced by connecting two tracks in parallel and simultaneously narrowing the aperture of both tracks [2]. If the structure contains more than three interdigital transducers (IDT), however, the topology of the connections becomes very complicated, or even impossible on the wafer level.

One-track filters with five transducers have been shown to provide good performance at high frequencies [3], [4]. A 5-IDT device features several advantages over, e.g., 3-IDT devices, such as a wider achievable passband and reduced resistive losses owing to the smaller optimal aperture required for matching to the load impedance. In order to further reduce the ohmic losses, it would be advantageous to reduce the aperture. An evident solution is to connect two tracks in parallel [2]. However, as stated above, for 5-IDT CRFs the parallel connection of two tracks is not straightforward, and other means of reducing the insertion loss must be found. In this paper, we show that replacing the gaps between the transducers with short transducers reduces the insertion loss of the device. The phase change is realized in the short transducer sections between the main transducers—in total, we use 13 transducers—and the structure is closer to synchronous. Effectively, the gap is distributed over the short transducers. This reduces the insertion loss as the scattering from the gap into bulk waves and the free-surface propagation attenuation are reduced. Also, the optimal aperture becomes narrower as the total number of fingers increase, further reducing the resistive losses in electrodes. We use leaky waves on 42°-lithium tantalate ($LiTaO_3$), a cut that in terms of propagation loss is optimum for leaky-wave propagation in a grating with a metal thickness of 0.07–0.1$\lambda$, but it is not optimum for propagation on a free or uniformly metallized surface [5]. A similar approach is disclosed in [6]. The device operates with unbalanced input and balanced output.

In this paper, we also discuss the effect of the layout of the contact pads and the connections on the performance and the balance characteristics of the device. At high frequencies, the effect of the capacitance between the contact pads increases and may strongly distort the response of the device. Therefore, the layout of the device must be chosen such that the parasitic capacitances arising from the connections and the contact pads are minimized.

The metallized-gap devices at the center frequency of 1842 MHz discussed in [3] and [4] feature an insertion loss of approximately 2 dB in the passband. We report experimental results for a distributed-gap device on 42°-$LiTaO_3$, at 1842 MHz. A wide bandwidth of 4.5% and a suppression level of −40 dB are achieved. The best devices feature a minimum insertion loss of <1 dB and maximum insertion loss of 1.2 dB in the passband. The passband is very flat, with a ripple <1 dB.

## II. Computational Results

### A. Theoretical Framework

For the optimization of the structure, we use a design software that uses the coupling-of-modes (COM) model (see, e.g., [7]) and transmission matrices [8]. Each element of the device—transducer, reflector, and gap—is described

Manuscript received May 17, 2004; accepted September 9, 2004.

The authors are with the Materials Physics Laboratory, Helsinki University of Technology, (Technical Physics), FIN-02015 HUT, Finland (e-mail: Johanna.Meltaus@hut.fi).

V. P. Plessky and S. Härmä also are with GVR Trade SA, CH-2022 Bevaix, Switzerland.

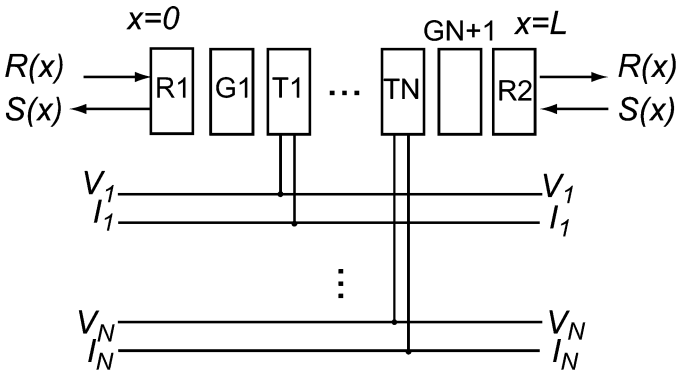


Fig. 1. Schematic of an N-port CRF device represented with transmission matrices. Each element (R for reflector, G for gap, and T for transducer) is described with a transmission matrix. The transducers are connected to the N electrical ports. In addition to the electric ports, the structure has two acoustic ports. The SAW field is described by the two counter-propagating modes $R$ and $S$.

with a transmission matrix that relates the acoustic fields, voltage, and current at the beginning of the element to the same quantities at the end of the device. The elements of the matrices are calculated by solving the COM equations:

$$\begin{cases} \dfrac{dR(x)}{dx} = -j\delta R(x) - j\kappa S(x) + j\alpha V \\ \dfrac{dS(x)}{dx} = j\kappa^* R(x) + j\delta S(x) - j\alpha^* V \\ \dfrac{dI(x)}{dx} = -2j\alpha^* R(x) - 2j\alpha S(x) + j\omega C V \end{cases}, \quad (1)$$

where $R(x)$ and $S(x)$ are slowly varying acoustic fields, $V$ and $I$ are the voltage and the current in the device, respectively, and $\delta$, $\kappa$, and $\alpha$ are the COM parameters.

The transmission matrix for a transducer connected to port 1 in a two-port system is of the form

$$\begin{pmatrix} R(x_2) \\ S(x_2) \\ V_1(x_2) \\ I_1(x_2) \\ V_2(x_2) \\ I_2(x_2) \end{pmatrix} = \begin{pmatrix} F_{11} & F_{12} & F_{13} & 0\,0\,0 \\ F_{21} & F_{22} & F_{23} & 0\,0\,0 \\ 0 & 0 & 1 & 0\,0\,0 \\ -F_{31} & -F_{32} & -F_{33} & 1\,0\,0 \\ 0 & 0 & 0 & 0\,1\,0 \\ 0 & 0 & 0 & 0\,0\,1 \end{pmatrix} \begin{pmatrix} R(x_1) \\ S(x_1) \\ V_1(x_1) \\ I_1(x_1) \\ V_2(x_1) \\ I_2(x_1) \end{pmatrix}, \quad (2)$$

where $x_1$ denotes the beginning of the transducer element and $x_2$ is the end of the element. Transmission matrix elements $F_{ij}$ are calculated from the solution of (1). The quantities $V_1$, $V_2$, $I_1$, and $I_2$ denote the voltages and currents in ports 1 and 2, respectively. The total matrix of a general N-port structure such as shown in Fig. 1 is obtained by cascading the element matrices. Although in Fig. 1 only one transducer is connected to a specified electric port, in principle several transducers may be connected to a single port. In addition to the N electric ports, the structure has two acoustic ports, one at $x = 0$ and the other at $x = L$, where $L$ is the total length of the device. The surface acoustic wave propagating within the structure is described in terms of two counter-propagating modes, $R$ and $S$. For an N-port device, the total transmission matrix is of size $(2N + 2) \times (2N + 2)$.

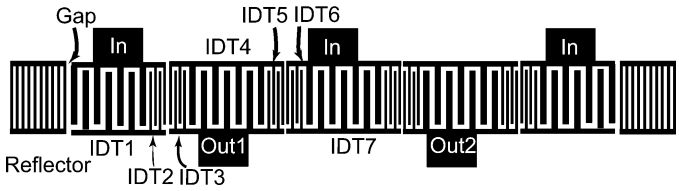


Fig. 2. Schematic of the 5-IDT filter with distributed gaps. All the gaps between IDTs are replaced with two short transducer sections. The structure is symmetric.

For simplicity, the COM simulations were performed for a corresponding single-ended structure, but the transmission-matrix method enables straightforward inclusion of balanced operation [9].

### *B. Device Structure*

The architecture of the device investigated here is a 5-IDT multimode longitudinally coupled resonator filter with distributed gaps. The device is symmetric and comprises five acoustically coupled main transducers and eight short transducer sections—13 transducers in total, as depicted in Fig. 2. The structure is quasisynchronous, i.e., there are no distinctive gaps between the transducers. The phase change required between the main transducers is produced with the short transducer sections at the ends of the main transducers (constituting the distributed gaps). Essentially, a certain number of fingers (six in our case) from each transducer is replaced with electrodes having a pitch different from the rest of the main transducer. The pitch is typically (but not necessarily) smaller than that of the main IDTs, in order to avoid scattering into bulk-acoustic wave modes. In our design, the pitches of the short sections are about 93% of the main IDT pitch. Distributing the necessary phase change over both of the transducers adjoining the gap, instead of replacing fingers in only one of them, makes it easier to keep the overall performance of the device unchanged. As Fig. 2 shows, the short transducer sections are electrically connected to the adjoining main IDT, such that the alternation of hot and ground electrodes is not disturbed. The gaps between reflectors and the first and the last IDT are not replaced, as they are typically close to synchronous anyway and do not have a significant effect on the operation of the device.

Because the device has five acoustically coupled transducers, there are at least three acoustic resonance modes contributing to the final filter response. Compared to, e.g., 3-IDT CRF structures, assembling the total response from a larger number of interacting modes enables a wider passband with reduced ripple.

The effect of the distributed gaps is to reduce both the scattering of SAW into bulk acoustic waves (BAW) and the propagation attenuation on free surface. Surface waves lose energy at the ends of periodic structures such as IDTs, as part of the wave is radiated into BAW modes [7]. Because the distributed gap structure has no distinct gaps, discontinuities in periodicity become less prominent, and

the BAW-radiation effect is reduced. Another source of loss, important especially at high frequencies, is the attenuation of the leaky waves propagating on 42°-$LiTaO_3$ on free or uniformly metallized surface. The $0.08\lambda$ metal thickness is close to the optimum, and the propagation loss is close to zero for a metal grating, whereas a uniform metallization increases it to approximately 0.008 dB/$\lambda$ [5]. The large number of gaps present in the design makes this effect significant.

The admittance of a CRF, and thus its matching to the load impedance, depends primarily on the capacitance of the structure, determined by the area of the filter. Because of the larger total number of fingers in the distributed-gap device compared with a traditional CRF, its aperture must be reduced in order to maintain the load-matching condition. The optimal aperture for the device studied in this paper is $35\lambda$, whereas the typical aperture of a 5-IDT CRF is about $60\lambda$. This yields a further reduction of loss, as the resistive losses in the electrodes are decreased. For the total reduction of loss, arising from all the effects described above, different estimates for 3-IDT devices yield an improvement in the passband insertion loss ranging from 0.4 dB to 1 dB [6], [10].

### *C. Distributions of Acoustic Power Flow*

We have designed an extremely wide-band 5-IDT filter with simulated response, shown with a solid line in Fig. 3(a), in order to study the acoustic wave power inside a distributed-gap device. The −3 dB absolute bandwidth is about 132 MHz (7%), which demonstrates that this approach yields record-high values of passband width compared to other CRF designs. The frequency response is formed by three distinct resonance peaks. The peaks are revealed at mismatched system impedances. For a device designed to operate with 50 Ω in the input and 150 Ω in the output, the situation with 1-Ω environment is illustrated in Fig. 3(a) with a dashed line.

We calculated the acoustic power-flow distribution over the length of the device at five frequency points: the three resonance frequencies [notated fr1, fr2, and fr3 in Fig. 3(a)], and the two intermediate frequencies [fi1 and fi2 in Fig. 3(a)]. The approximate frequencies for these points are fr1 ≈ 1789 MHz, fi1 ≈ 1806 MHz, fr2 ≈ 1830 MHz, fi2 ≈ 1876 MHz, and fr3 ≈ 1914 MHz. The power flows shown on the left column in Fig. 3 were calculated in matched 50/150-Ω environment, and the power flows on the right column were calculated in 1-Ω environment.

The acoustic power distributions show that the acoustic power flows have significantly different distributions along the structure at different frequency points of the passband. In particular, at fr2 we have a more or less uniform distribution of energy over the whole device, but at fr3 the resonances are confined into the area inside and in the vicinity of the short reflectors. In the frequencies where SAW power flows are the most intensive near and inside the distributed gaps (fi2, fr3), the SAW energy is rather uniformly distributed in the regions of the main transducers. In Fig. 3(f), the undulating distribution in the reflectors shows that this frequency is already at the limit of the stopband of the reflectors.

### *D. Simulation Results for a DCS Rx Filter*

For the actual device to be used as a digital cellular system (DCS) Rx filter, we produced another design with the frequency response (shown in Fig. 4) satisfying one of the most demanding specifications for this kind of application. The result of the COM simulation is depicted in Fig. 4 with a dashed line, together with the experimental curve indicated by the solid line. The device operates at the center frequency of 1842 MHz. The simulated 3-dB bandwidth is 85 MHz (4.6%), the minimum insertion loss is 0.95 dB and the ripple in the passband is minimal. Suppressions outside the passband are at −40 dB level on the left side of the passband and at −30 dB level on the right side. The gently sloping skirts on this side are typical for CRF architecture. To improve the skirts on the right-hand side, an external synchronous resonator may be coupled as an impedance element, as is done, e.g., in [3].

## III. Experimental Results

The 5-IDT CRF filter simulated in Fig. 4 (dashed line) was fabricated and measured. The substrate material was 42°-$LiTaO_3$, with aluminum thickness of $0.08\lambda$ (1870 Å). Two layouts, depicted in Fig. 5, were implemented: Layout 1 had separate grounds for input and output and the contact pads for input and output were on different sides of the device. Layout 2 had all grounds connected and all contact pads on the same side of the device. The distance between input and output contact pads was approximately 450 $\mu$m for Layout 1 and 105 $\mu$m for Layout 2. Both layouts were probed directly on wafer.

The solid line in Figs. 4 and 6 shows a typical experimental curve for the 5-IDT device with type 1 layout (separate grounds, contact pads on different sides of the filter). A matching inductance of 30 nH was added at the output when processing the measured data so as to improve the matching to the 150 Ω load because, for such a wide passband, it is extremely difficult to obtain low loss without matching. The small ripple seen on the measurement curve is due to the measurement setup, and its origin is not quite clear.

The agreement with the simulated response is excellent, as seen in Fig. 4. In the simulation, we have included some parasitics such as tip resistance, but their values were approximations and were not fitted to the measurements. The experimental 2.5-dB passband width is 83 MHz (4.5%), the minimum insertion loss is 0.6 dB, and the ripple in the passband is below 1 dB. Suppressions are at −40-dB level on the left-hand side of the passband and go down to −30-dB level on the right-hand side.

In Fig. 6, the measurement results for both layouts are shown, with a close-up of the passband as an inset. The results show that the overall shape of the response is rather

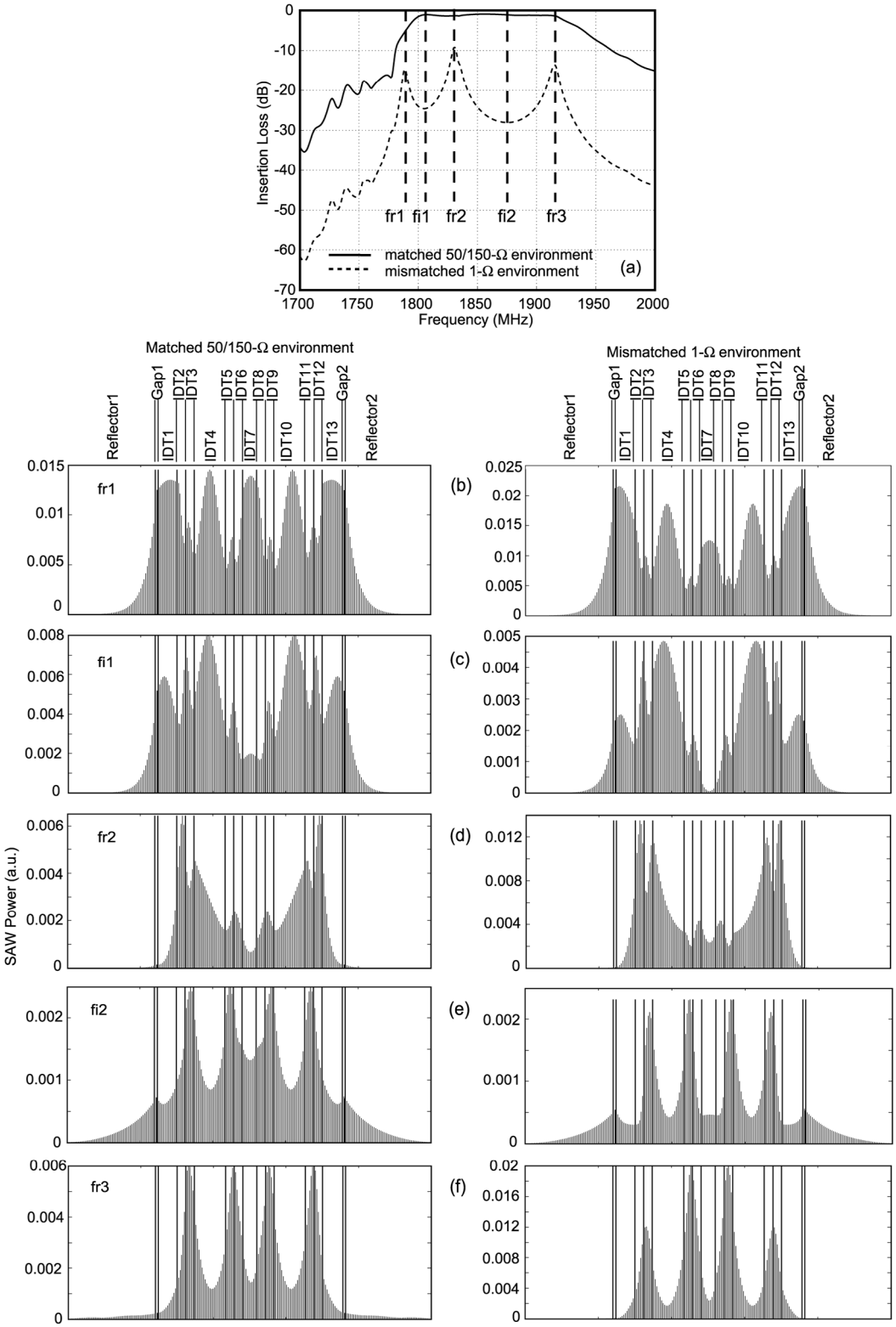


Fig. 3. Calculated acoustic power flow over an extremely wide-band, 5-IDT, distributed-gap device at five frequencies. (a) Simulated frequency response in the passband at matched (50/150 Ω, solid line) and mismatched (1 Ω, dashed line) load impedances. The acoustic power flow is shown at the frequencies marked with vertical lines in (a): the first, second, and third resonance frequencies [(b), (d), and (f), respectively] and the first and second intermediate frequencies [(c) and (e), respectively]. The figures on the left-hand side are calculated for the matched situation in 50/150-Ω environment, and those on the right are for the 1-Ω environment.

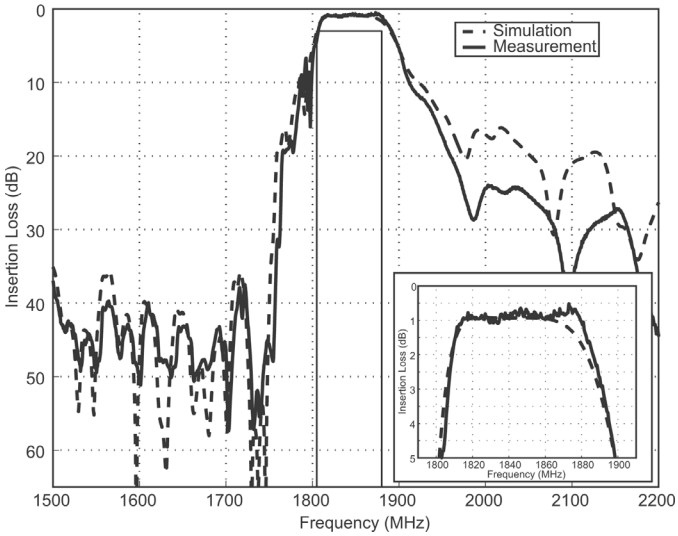


Fig. 4. COM simulation (dashed line) and measurement (solid line) of the 5-IDT, DCS Rx filter structure on 42°-$LiTaO_3$. The simulated response features an extremely flat passband, wide bandwidth, and high suppression levels. The agreement between simulation and measurement is excellent. The experimental response features a wide passband (4.5%), an extremely low loss (<1 dB), a very small ripple (<1 dB), and high suppression levels.

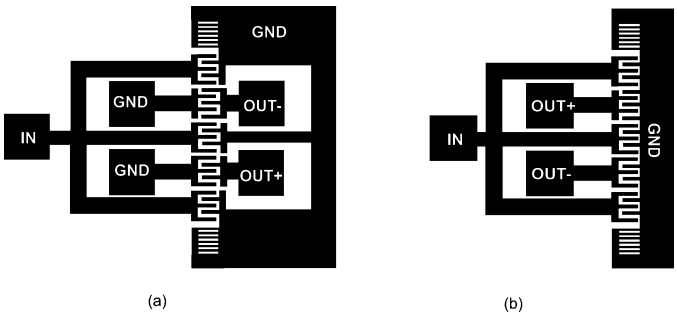


Fig. 5. Schematics of the two proposed layouts. Layout 1 (a) has the input and output contact pads on opposite sides of the filter track. Moreover, input and output grounds are separated. The distance between the input and output pads is approximately 450 $\mu$m. Layout 2 (b) has a common ground for input and output and the contact pads are situated on the same side of the filter track. The distance between the input and output contact pads is approximately 110 $\mu$m.

similar for both device layouts. However, Layout 2 introduces a small additional insertion loss in the passband, in addition to which the passband is 4 MHz narrower. Moreover, the transmission curves in the suppression region on the left side of the passband are different for the two layouts, although both layouts yield approximately the same suppression levels. Both effects are interpreted to originate from additional feedthrough in Layout 2, caused by the small distance between the input and output contact pads. However, it must be noted here that the two layouts required different sets of probe tips for the 3-port measurements. Thus, the possibility of minor calibration errors between the two measurements, due to the need to readjust and recalibrate the measurement setup, is not to be excluded.

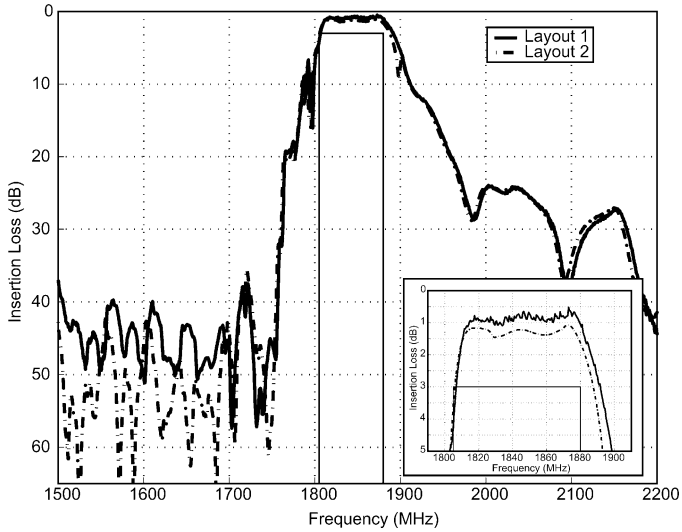


Fig. 6. Experimental results for two different layouts: solid curve: Layout 1, dash-dotted curve: Layout 2. Layout 2 introduces changes in the shape of the frequency responses in the passband and on the left-hand side of the passband. The inset shows a close-up of the passband, with Layout 1 depicted with the solid curve and Layout 2 with the dash-dotted curve.

In Fig. 7, the amplitude and phase balance for both layouts are compared. It is seen that, for Layout 1, amplitude imbalance is between 0 dB and 1 dB, and for Layout 2, it is between −1.9 dB and 1.4 dB. Similarly, for phase difference, Layout 1 yields values between −5° and 8°, and Layout 2 generates a phase balance between −8° and 8°. Moreover, both the amplitude and the phase imbalance for Layout 2 vary considerably faster than those for Layout 1. The larger imbalance is due to the increased capacitance between the input and output contact pads situated close to each other.

## IV. Conclusions

We have designed, fabricated, and measured a 5-IDT longitudinally coupled resonator filter with additional two six-finger IDTs with reduced pitch replacing the gaps of the traditional design. The device operates at a center frequency of 1842.5 MHz with unbalanced input and balanced output. The filter features excellent agreement with simulations, extremely low loss in the passband, wide bandwidth, and high suppression levels.

When distributed gaps are used instead of conventional metallized gaps, several mechanisms contribute to the reduction of loss in the device. The attenuation arising from the scattering of SAW energy into bulk acoustic waves at the discontinuities of periodicity is significantly decreased. The attenuation of leaky waves on free or uniformly metallized surface of 42°-$LiTaO_3$ is reduced. Moreover, the resistive losses in the electrodes decrease as the optimal aperture of the device is reduced as a consequence of the increased total number of electrodes. These effects yield improved performance in the passband.

We investigated experimentally the effect of the contact pad layout on the filter performance. At high frequencies,

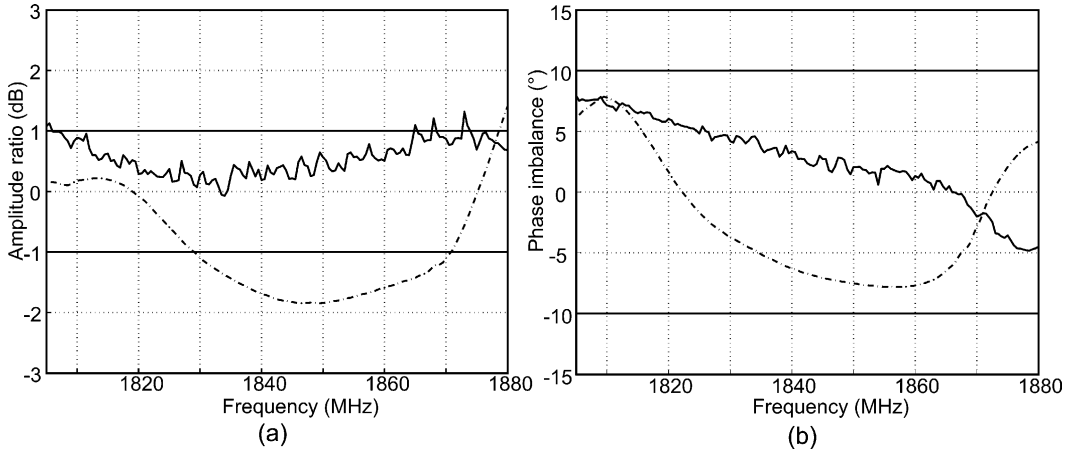


Fig. 7. Experimental results for (a) amplitude and (b) phase balance for the two different layouts depicted in Fig. 4. Solid curve: Layout 1, dash-dotted curve: Layout 2. Layout 2 gives amplitude and phase imbalance that varies faster than that for Layout 1.

the parasitic capacitance between the input and output contact pads has a strong effect on the filter response. We conclude that separating the input and output grounds and contact pads yields improved performance in terms of passband insertion loss, passband width and amplitude and phase balance.

The 5-IDT filter architecture with distributed gaps is an interesting approach to improving CRF response. It is advantageous in applications requiring a wide band with extremely low loss in the passband, especially if 42°-$LiTaO_3$ is used as the substrate material. At high frequencies, the pad layout must be optimized for minimal interference with the filter performance.

## Acknowledgment

J. M. thanks the Finnish Cultural Foundation for a postgraduate scholarship. We thank P. Brown for measuring the devices and W. Bonner for processing the measurement data.

## References

[1] T. Morita, Y. Watanabe, M. Tanaka, and Y. Nakazawa, "Wide-band low loss double mode SAW filters," in *Proc. IEEE Ultrason. Symp.*, 1992, pp. 95–104.

[2] J. Meltaus, V. P. Plessky, A. Gortchakov, S. Härmä, and M. M. Salomaa, "SAW filter based on parallel-connected CRFs with offset frequencies," in *Proc. IEEE Ultrason. Symp.*, 2003, pp. 2073–2076.

[3] M. Koshino, K. Kanasaki, N. Akahori, R. Chujyo, and Y. Ebata, "A wide-band balanced SAW filter with longitudinal multi-mode resonator," in *Proc. IEEE Ultrason. Symp.*, 2000, pp. 387–390.

[4] S. Ichikawa, H. Kanasaki, N. Akahori, M. Koshino, and Y. Ebata, "Mode analysis of longitudinal multi mode SAW resonator filter," in *Proc. IEEE Ultrason. Symp.*, 2001, pp. 101–106.

[5] O. Kawachi, S. Mineyoshi, G. Endoh, M. Ueda, O. Ikata, K. Hashimoto, and M. Yamaguchi, "Optimal cut for leaky SAW on $LiTaO_3$ for high performance resonators and filters," *IEEE Trans. Ultrason., Ferroelect., Freq. Contr.*, vol. 48, pp. 1442–1448, Sep. 2001.

[6] T. Bauer, G. Kovacs, U. Rösler, and W. Ruile, "Surface acoustic wave arrangement with a junction region between surface acoustic wave structures having a decreasing then increasing finger period," U.S. Patent 6,420,946, July 2002.

[7] V. P. Plessky and J. Koskela, "Coupling-of-modes analysis of SAW devices," *Int. J. High Speed El. Syst.*, vol. 10, pp. 1–81, Dec. 2000.

[8] K.-Y. Hashimoto, *Surface Acoustic Wave Devices in Telecommunications: Modelling and Simulation*. Berlin: Springer-Verlag, 2000.

[9] M. Koshino, H. Kanasaki, T. Yamashita, S. Mitobe, M. Kawase, Y. Kuroda, and Y. Ebata, "Simulation modeling and correction method for balance performance of RF SAW filters," in *Proc. IEEE Ultrason. Symp.*, 2002, pp. 301–305.

[10] W. Wang, X. Zhang, H. Wu, Y. Shui, and V. P. Plessky, "On minimizing bulk scattering loss in CRF(DMS) devices," in *Proc. IEEE Ultrason. Symp.*, 2004, pp. 1363–1366.

**Johanna Meltaus** was born in Espoo, Finland, in 1976. She received her Master of Science (in Technology) degree at Helsinki University of Technology (TKK), Espoo, Finland, in 2000, majoring in materials physics, and her Licentiate of Technology degree at TKK in 2002.

She has worked as a research assistant in the Low Temperature Laboratory (TKK) and in the Materials Physics Laboratory (TKK), and as a research scientist in the Materials Physics Laboratory, (TKK). She is currently working on her Dr.Tech. thesis in the Materials Physics Laboratory, TKK. Her previous research interests have included high-temperature superconducting devices and radio holography. Currently she is involved in designing and modeling coupled surface acoustic wave filters.

Ms. Meltaus was a corecipient of the Master's Thesis award of the Finnish Association of Graduate Engineers in 2001.

**Victor P. Plessky** (M'93–SM'01) received his Ph.D. degree in physical and mathematical sciences at the Moscow Physical-Technical Institute, Moscow, Russia, and the Dr.Sc. degree at the Institute of Radio Engineering and Electronics (IRE, Russian Academy of Sciences, Moscow), in 1978 and 1987, respectively. Beginning in 1978, he worked at IRE, first as a junior researcher and, in 1987, he was promoted to the position of Laboratory Director. In 1991, he also worked as a part-time professor at the Patris Lumumba University, Moscow.

He received the full professor title in 1995 from the Russian Government. In 1992, he joined ASCOM Microsystems SA in Bevaix, Switzerland, where he worked as a special SAW projects manager. Since 1997, he has lectured several courses on various SAW topics at Helsinki University of Technology (TKK), Espoo, Finland, as a visiting professor. Currently, he holds a docentship at TKK. Since 1998 he has been working at the Neuchatel office (Switzerland) of Thomson Microsonics (later Thales Microsonics, presently Temex Microsonics), and from 2002 as a consultant. He has been engaged in research on semiconductor physics, SAW physics (new types of waves, scattering and reflection on surface irregularities, laser generation of SAW), SAW device development (filters, delay lines, reflective array compressors), and magnetostatic wave studies.

Dr. Plessky's current interests focus on SAW physics and low-loss SAW filter development. He is an IEEE Senior Member. He was awarded the USSR National Award for Young Scientists in 1984.

**Sanna Härmä** was born in Kotka, Finland, in 1977. She received a Master of Science (in technology) degree in materials physics at Helsinki University of Technology (TKK), Espoo, Finland, in 2001, and has completed the pedagogical studies for teachers.

She has worked as a research assistant in the Laboratory of Biomedical Engineering (TKK) and in the Materials Physics Laboratory (TKK). After her graduation, she worked as a design engineer at Thales Microsonics, Sophia-Antipolis, France, and as a subject teacher of mathematics and physics in Helsinki, Finland. Currently, she is preparing her Dr.Tech. thesis in the Materials Physics Laboratory, TKK.

**Martti M. Salomaa** (M'95) received his Dr.Tech. degree in technical physics from Helsinki University of Technology (TKK), Espoo, Finland, in 1979. Thereafter, he worked at the University of California, Los Angeles (UCLA) and the University of Virginia, Charlottesville, VA. From 1982 to 1991, he was the theory group leader at the Low Temperature Laboratory, TKK, and from 1988 to 1991, he served as the Director of the Rotating Superfluid 3He research project between the Academy of Finland, Helsinki, Finland, and the Soviet Academy of Sciences, Moscow, Russia. He has held a sabbatical stipend at the University of Karlsruhe, Karlsruhe, Germany, and, in 1994, he was a guest professor at the Swiss Federal Institute of Technology (ETH)-Zurich, Switzerland. After 1996, he was a professor of technical physics and the Director of the Materials Physics Laboratory, Department of Engineering Physics and Mathematics, TKK. Professor Salomaa passed away on December 9, 2004.

Dr. Salomaa was a corecipient of the 1987 Award for the Advancement of European Science (presented by the Körber Foundation, Hamburg). His research interests included Bose-Einstein condensation, superfluidity, superconductivity, magnetism, physics of SAW, nondiffracting waves, nanoelectronics, mesoscopic physics and sonoluminescence. He was a member of the IEEE, the American Physical Society, the European Physical Society, and the Finnish Physical and Optical Societies.